

RAPID REPORT

Intermittent hypoxia during recovery from neonatal hyperoxic lung injury causes long-term impairment of alveolar development: A new rat model of BPD

Anastasiya Mankouski,^{1,2} Crystal Kantores,² Mathew J. Wong,^{2,4} Julijana Ivanovska,² Amish Jain,^{3,4} Eric J. Benner,¹ Stanley N. Mason,¹ A. Keith Tanswell,^{2,3,4} Richard L. Auten,¹ and Robert P. Jankov^{2,3,4}

¹Division of Neonatology, Department of Pediatrics, Neonatal-Perinatal Research Institute, Duke University Medical Center, Durham, North Carolina; ²Physiology & Experimental Medicine Program, Hospital for Sick Children Research Institute, Toronto, Ontario, Canada; ³Faculty of Medicine, Department of Pediatrics, University of Toronto, Toronto, Ontario, Canada; and ⁴Faculty of Medicine, Department of Physiology, University of Toronto, Toronto, Ontario, Canada

Submitted 13 October 2016; accepted in final form 30 November 2016

Mankouski A, Kantores C, Wong MJ, Ivanovska J, Jain A, Benner EJ, Mason SN, Tanswell AK, Auten RL, Jankov RP. Intermittent hypoxia during recovery from neonatal hyperoxic lung injury causes long-term impairment of alveolar development: A new rat model of BPD. *Am J Physiol Lung Cell Mol Physiol* 312: L208–L216, 2017. First published December 2, 2016; doi:10.1152/ajplung.00463.2016.—Bronchopulmonary dysplasia (BPD) is a chronic lung injury characterized by impaired alveologenesis that may persist into adulthood. Rat models of BPD using varying degrees of hyperoxia to produce injury either cause early mortality or spontaneously recover following removal of the inciting stimulus, thus limiting clinical relevance. We sought to refine an established rat model induced by exposure to 60% O₂ from birth by following hyperoxia with intermittent hypoxia (IH). Rats exposed from birth to air or 60% O₂ until day 14 were recovered in air with or without IH (FI_{O₂} = 0.10 for 10 min every 6 h) until day 28. Animals exposed to 60% O₂ and recovered in air had no evidence of abnormal lung morphology on day 28 or at 10–12 wk. In contrast, 60% O₂-exposed animals recovered in IH had persistently increased mean chord length, more dysmorphic septal crests, and fewer peripheral arteries. Recovery in IH also increased pulmonary vascular resistance, Fulton index, and arterial wall thickness. IH-mediated abnormalities in lung structure (but not pulmonary hypertension) persisted when reexamined at 10–12 wk, accompanied by increased pulmonary vascular reactivity and decreased exercise tolerance. Increased mean chord length secondary to IH was prevented by treatment with a peroxynitrite decomposition catalyst [5,10,15,20-Tetrakis(4-sulfonatophenyl)-21H,23H-porphyrin iron (III) chloride, 30 mg/kg/day, days 14–28], an effect accompanied by fewer inflammatory cells. We conclude that IH during recovery from hyperoxia-induced injury prevents recovery of alveologenesis and leads to changes in lung and pulmonary vascular function lasting into adulthood, thus more closely mimicking contemporary BPD.

chronic neonatal lung injury; bronchopulmonary dysplasia; oxygen toxicity, pulmonary hypertension

DESPITE MANY ADVANCES in neonatal care that have led to improved survival of infants born extremely preterm, development of bronchopulmonary dysplasia (BPD) and associated

chronic pulmonary hypertension (PHT) remain common adverse outcomes in this population (32). A cardinal feature of contemporary BPD is an inhibition or arrest of alveolar development (9). Lung findings in fatal BPD typically include “emphysematous” distal lung structure with fewer lung units, areas of septal thickening, microvascular dysplasia/hypoplasia, and inflammation (9). Remodeling of pulmonary resistance arteries due to smooth muscle hyperplasia and distal extension of smooth muscle into normally nonmuscular arteries is a pathognomonic structural finding of associated chronic PHT (42).

Consequences of moderate-severe BPD include persistent emphysema-like lung changes with airway obstruction and respiratory insufficiency (25, 43, 47) leading to potentially lifelong morbidity [premature lung “aging” (33)] and an increased risk of severe comorbidities, including chronic, progressive PHT and poor neurodevelopmental outcomes (2, 3, 8, 34). Animal models have provided insights into the pathogenesis of BPD and/or associated PHT and the regulation of alveologenesis (19, 39). Chronic exposure of neonatal rats to hyperoxia is a clinically relevant injury (35), leading to changes in lung structure and function that mimic BPD (18). However, to maximize clinical relevance, abnormal lung pathology should persist into adult life. Limitations of current rat hyperoxia models are that they are either rapidly lethal [$>90\%$ O₂ for >7 days (16, 18)] or, as described herein, spontaneously recover upon removal from the inciting stimulus (60% O₂ for 14 days). Intermittent hypoxia (IH) is another clinically relevant injury, replicating severe desaturation episodes observed in infants with evolving or established BPD (27). In this study, we sought to refine a rat chronic lung injury model secondary to exposure to 60% O₂ by following the hyperoxia exposure with IH, hypothesizing that IH may prevent recovery and lead to changes in lung structure and function that persist into adulthood.

MATERIALS AND METHODS

Materials. Oxygen exposure chambers and automated controllers (OxyCycler model A84XOV) were from Biospherix (Parish, NY). Alcohols, organic solvents, paraformaldehyde, Permunt, and Superfrost/Plus microscope slides were from Fisher Scientific (Whitby, Ontario, Canada). Weigert’s resorcin-fuchsin stain was from Rowley

Address for reprint requests and other correspondence: R. P. Jankov, Hospital for Sick Children, 09.9707 Peter Gilgan Centre for Research and Learning, 686 Bay St., Toronto, ON, Canada M5G 0A4 (e-mail: robert.jankov@sickkids.ca).

Biochemical (Danvers, MA). Anti- α -smooth muscle actin (catalog no. MA1-12772) was from Thermo Scientific. Anti-myeloperoxidase; (catalog no. A0398) was from DAKO Agilent (Mississauga, Ontario, Canada). Anti-cluster of differentiation (CD) 68 (catalog no. MCA341R) was from Serotec (Raleigh, NC). Anti-nitrotyrosine (catalog no. 06-284) was from EMD Millipore (Billerica, MA). Avidin-biotin-peroxidase complex immunohistochemistry kits and 3,3'-diaminobenzidine staining kits were from Vector Laboratories (Burlingame, CA). Biotinylated goat anti-mouse IgG (catalog no. 14709) was from Cell Signaling Technologies (Beverly, MA). 5,10,15,20-Tetrakis(4-sulfonatophenyl)-21H,23H-porphyrin iron (III) chloride (FeTPPS) and peroxyntrite were from Cayman Chemical (catalog no. 17187; Ann Arbor, MI). Unless otherwise specified, all other chemicals and reagents were from Bioshop (Burlington, Ontario, Canada).

Injury model. The Animal Care Committee of the Hospital for Sick Children Research Institute approved this study. Timed-pregnant Sprague-Dawley rats were from Taconic Farms (Germantown, NY). Litters were born in the exposure chambers and continuously exposed to hyperoxia (60% O₂) or air (21% O₂) until *postnatal day* (PND) 14. To avoid potential confounding effects of sex misdistribution and variations in litter size, litters were adjusted on the day of birth to consist of 12 pups: 6 males and 6 females (sex identified by anogenital distance). To avoid maternal toxicity and consequent undernutrition of pups (16), dams were swapped daily between air and hyperoxia chambers. From PND 14, litters were recovered in air with or without IH (10% O₂ for 10 min every 6 h) until PND 28. This regimen did not cause mortality or growth restriction, which can independently augment lung injury (44). In preliminary experiments, intermittent 13% O₂ had no effect on lung injury, and longer (20-min) periods in 10% O₂ caused growth restriction (data not shown). For each exposure group, four litters were used (16 litters in total). From PND 28, 12 animals from each group (equal sex distribution) remained in room air until 10–12 wk of age. An additional eight litters (2 litters/exposure group) were treated with FeTPPS (30 mg·kg⁻¹·day⁻¹ daily ip; 4 litters) or 0.9% saline vehicle (4 litters), as previously described (28), from PND 14 to 28. A schematic illustration of the injury model and interventions is provided in Fig. 1.

Pulmonary vascular resistance. Two-dimensional echocardiography and pulsed-wave Doppler ultrasound were performed as previously described (23). To evaluate pulmonary vascular reactivity, measurements were made after a 5-min exposure to 10% O₂.

Right ventricular hypertrophy. Right ventricular hypertrophy (RVH) was quantified using the Fulton index (right ventricle/left ventricle + septum dry weight ratio), as previously described (23).

Exercise tolerance. Adult rats (10–12 wk of age) were trained daily on an Exer-3/6 animal treadmill (Columbus Instruments, Columbus, OH) over a 7-day period, as previously described (46).

Histological studies. Lungs from six animals from each group (1 male and 1 female from each of 3 separate litters) were air-inflated and perfusion-fixed at constant pressure, embedded in paraffin, sectioned, and stained with hematoxylin-eosin, for elastin, or immunostained for inflammatory cells, as previously described (23, 31, 36). For all analyses, measurements were carried out on four noncontiguous left lung sections per animal by an observer blinded to group

identity. Analysis of mean chord length (L_m), tissue fraction, counts of peripheral arteries (vessels of external diameter 20–65 μ m with both internal and external elastic laminae visible), and counts of elastin-stained secondary crests were conducted as previously described (28, 31, 36) from 10 random nonoverlapping low-power fields imaged from each section. L_m was normalized to lung volume, quantified by water displacement (24). Tissue fraction normalized to lung volume, a measure of the volumetric proportion of tissue compared with total area, was performed using the point-counting method, as described by Weibel (45). Septal crests were considered dysmorphic if elastin at the septal tip was frayed (vs. compact and dense for normal crests). Measurement of arterial medial wall area, arterial muscularization, immunostaining for 3-nitrotyrosine, CD68, and myeloperoxidase, and inflammatory (macrophage and neutrophil) cell counts were all performed as previously described (11, 13, 26, 46). A nitrotyrosine staining index, representing the percentage of tissue area reaching a preset staining intensity threshold (normalized to tissue area), was derived as previously described in detail (11).

Data presentation and statistical analysis. Values are shown as means \pm SE. Analyses were performed using Sigma Plot 12.5 (Systat Software, San Jose, CA). Statistical significance was determined by one- or two-way ANOVA, then using Tukey's post hoc test, where significant ($P < 0.05$) intergroup differences were found.

RESULTS

Recovery in IH alters lung morphology. Exposure to 60% O₂ for 14 days leads to decreased numbers of secondary crests and peripheral vessels (31). As shown in Fig. 2, these changes were no longer present after recovery in air until PND 28. Recovery in IH caused no significant changes in body weight, wet lung weight, or lung volume (measured by displacement) at PND 28 (data not shown). Recovery of 60% O₂-exposed animals in IH prevented recovery of alveologenesis, as measured by increased L_m (Fig. 2A) and decreased tissue fraction (Fig. 2B). In addition, we observed fewer peripheral arteries (Fig. 2C) and nondysmorphic secondary crests (Fig. 2F) and more dysmorphic secondary crests (Fig. 2F). Interestingly, IH in animals exposed to air from PND 1 to 14 also caused smaller, but significant, changes in L_m (Fig. 2A), tissue fraction (Fig. 2B), and numbers of peripheral arteries (Fig. 2C).

Recovery in IH causes PHT. Exposure to 60% O₂ for 14 days leads to changes of PHT, including arterial wall thickening and RVH (31). These changes were no longer present after recovery in air until PND 28 (Fig. 3). In contrast, recovery of 60% O₂-exposed animals in IH increased the pulmonary vascular resistance (PVR) index (Fig. 3A), RVH (Fig. 3B), arterial medial wall area (Fig. 3C), and increased numbers of fully muscularized arteries (Fig. 3E). IH in animals exposed to air from PND 1 to 14 also increased arterial medial wall area (Fig. 3B), whereas increases in

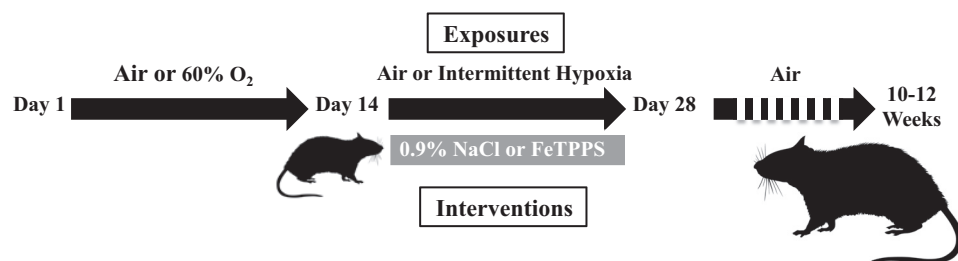


Fig. 1. Schematic illustration of exposures and interventions.

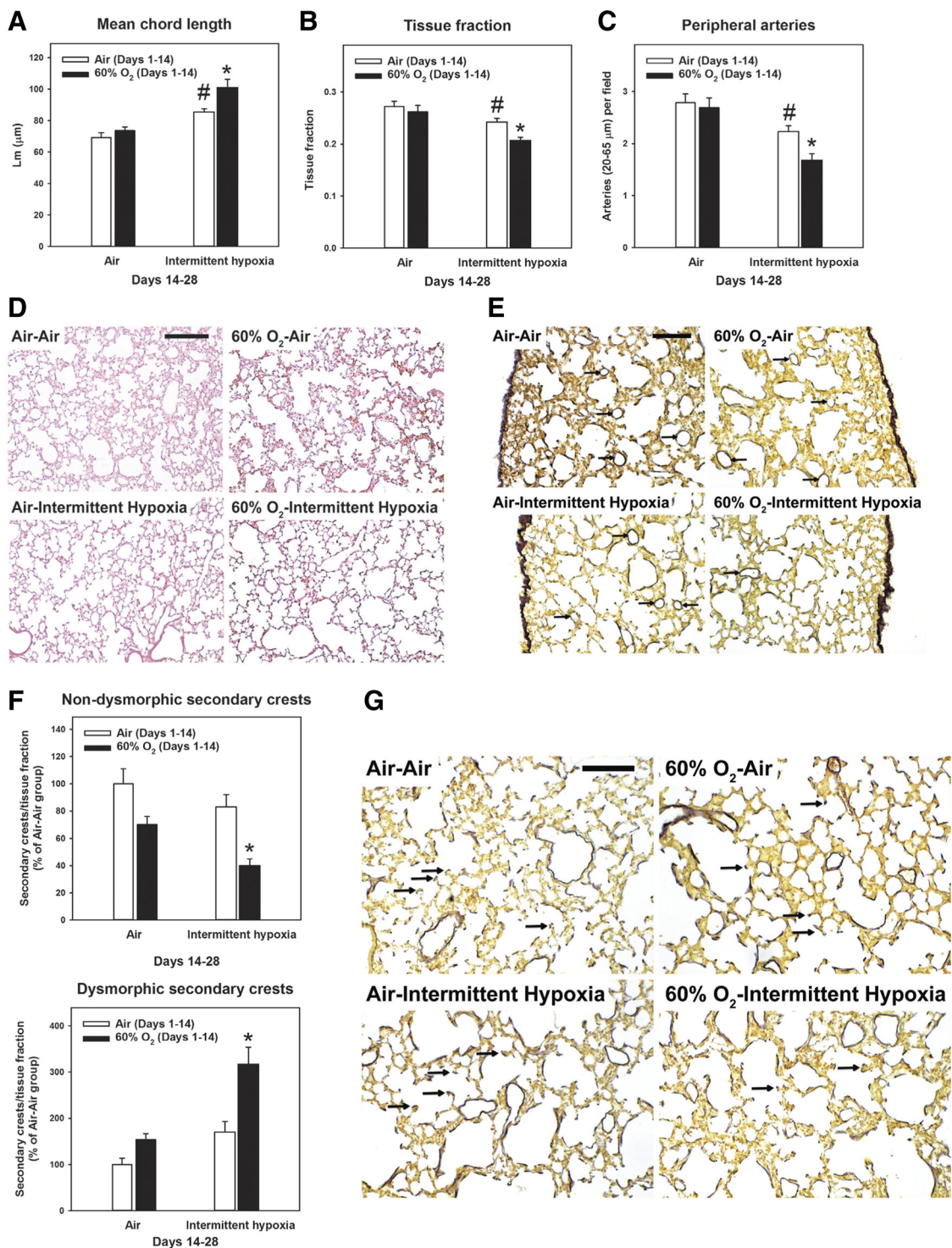


Fig. 2. Changes in lung morphology secondary to intermittent hypoxia. Rat pups were exposed to normoxia (Air; open bars) or hyperoxia (60% O₂; closed bars) from *postnatal days 1 to 14* followed by recovery in normoxia (Air) or intermittent hypoxia (Intermittent hypoxia) until *postnatal day 28*. A—C: morphometric analyses of mean chord length (A), tissue fraction (B), and peripheral artery counts (C) ($n = 6$ animals/group). D and E: representative photomicrographs of hematoxylin and eosin (D) (bar length = 250 μm) and elastin-stained sections (E) (bar length = 100 μm). Arrows point to peripheral arteries. F: counts of normal and dysmorphic secondary crests ($n = 4-5$ animals/group). G: representative photomicrographs of elastin-stained sections with arrows pointing to secondary crests. Bar length = 100 μm . Graph bars represent means \pm SE * $P < 0.05$, by ANOVA, compared with all other groups. # $P < 0.05$, by ANOVA, compared with Air-Air group.

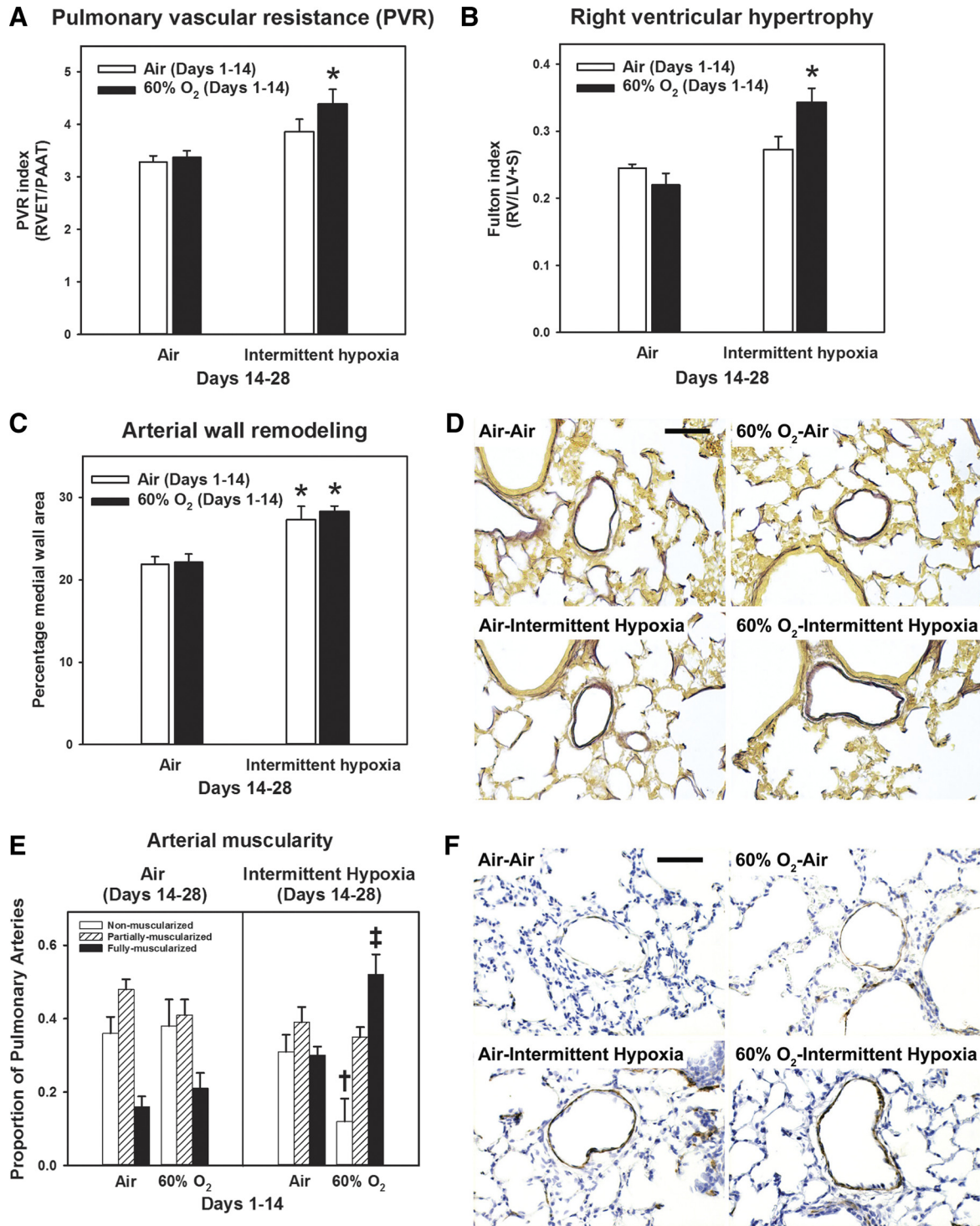


Fig. 3. Changes in markers of pulmonary hypertension secondary to intermittent hypoxia. Rat pups were exposed to normoxia (Air) or hyperoxia (60% O₂) from *postnatal days 1 to 14* followed by recovery in normoxia (Air) or intermittent hypoxia (Intermittent hypoxia) until *postnatal day 28*. *A*: pulmonary vascular resistance index ($n = 11-12$ animals/group). *B*: Fulton index (right ventricular hypertrophy; $n = 6$ animals/group). *C*: percentage medial wall area (arterial wall remodeling; $n = 6$ animals/group). *D*: representative high-power photomicrographs of elastin-stained pulmonary arteries (bar length = 50 μm). *E*: muscularization of pulmonary arteries ($n = 4-5$ animals/group). *F*: representative high-power photomicrographs of α -smooth muscle actin-stained pulmonary arteries (bar length = 50 μm). Graph bars represent means \pm SE. * $P < 0.05$, by ANOVA, compared with Air-Air and 60% O₂-Air groups. † $P < 0.05$, by ANOVA, for nonmuscular arteries, compared with Air-Air and 60% O₂-Air groups. ‡ $P < 0.05$, by ANOVA, for fully muscularized arteries compared with all other groups.

PVR (Fig. 3A) and the proportion of fully muscularized arteries (Fig. 3E) were not significant.

Recovery in IH causes long-term changes in lung structure, pulmonary vascular reactivity, and exercise capacity. Morphometric analyses were conducted on animals between 10 and 12 wk of life (young adulthood) following recovery in room air from PND 28 (Fig. 4). Young adult animals that were exposed to 60% O₂-IH had persistently increased L_m (Fig. 4A) and fewer peripheral arteries (Fig. 4B). As young adults, animals

exposed to 60% O₂-IH no longer had evidence of PHT [PVR and Fulton indexes were comparable to air-exposed controls ($P > 0.05$); data not shown]. However, there was increased pulmonary vascular reactivity, shown by a greater PVR index in response to acute hypoxia (Fig. 4D), in animals who recovered in IH, whether or not they were initially exposed to hyperoxia. As previously reported (46), female rats ran a greater distance compared with male rats across all groups; therefore, data were stratified by sex. Exercise capacity was

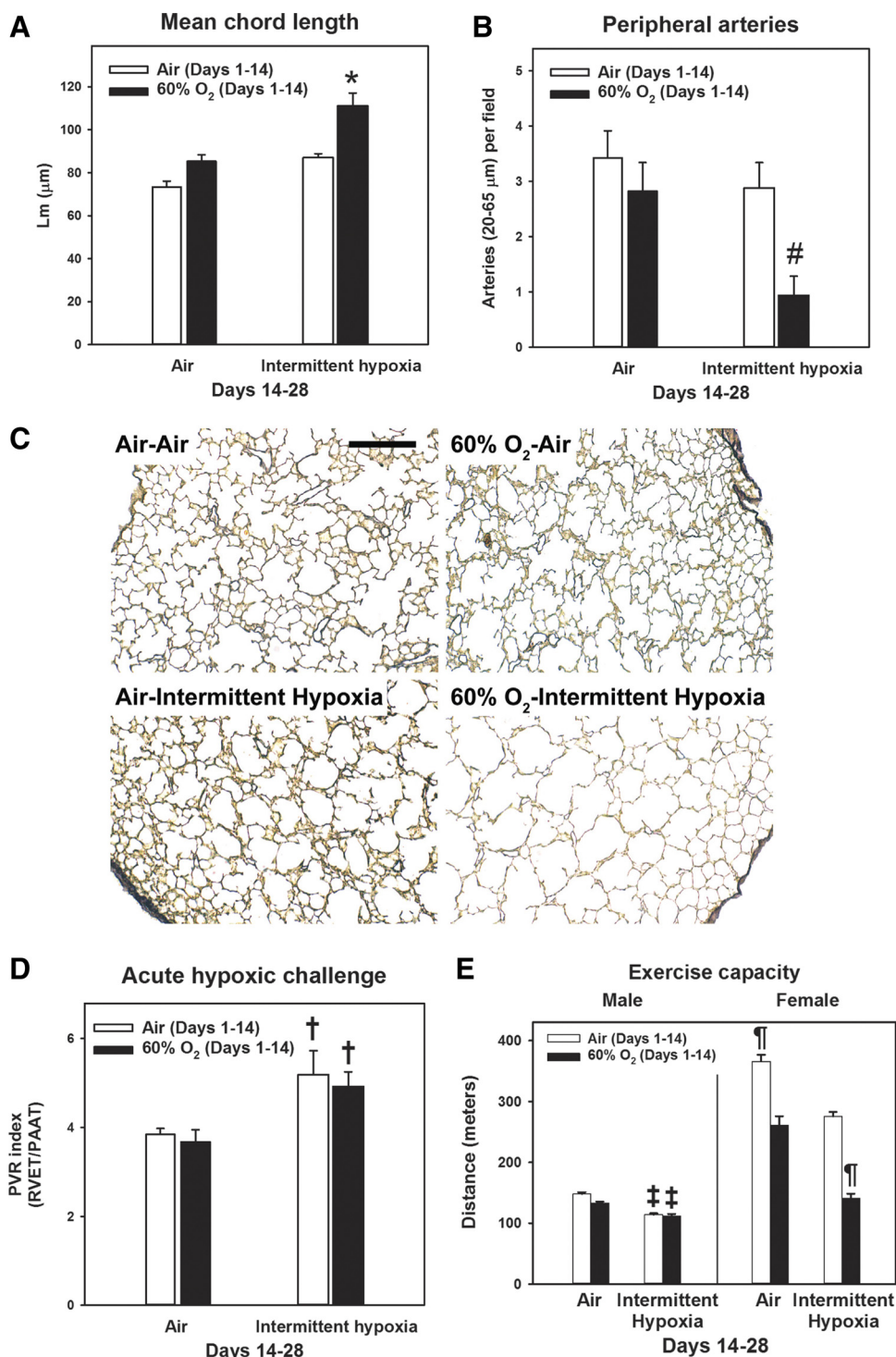
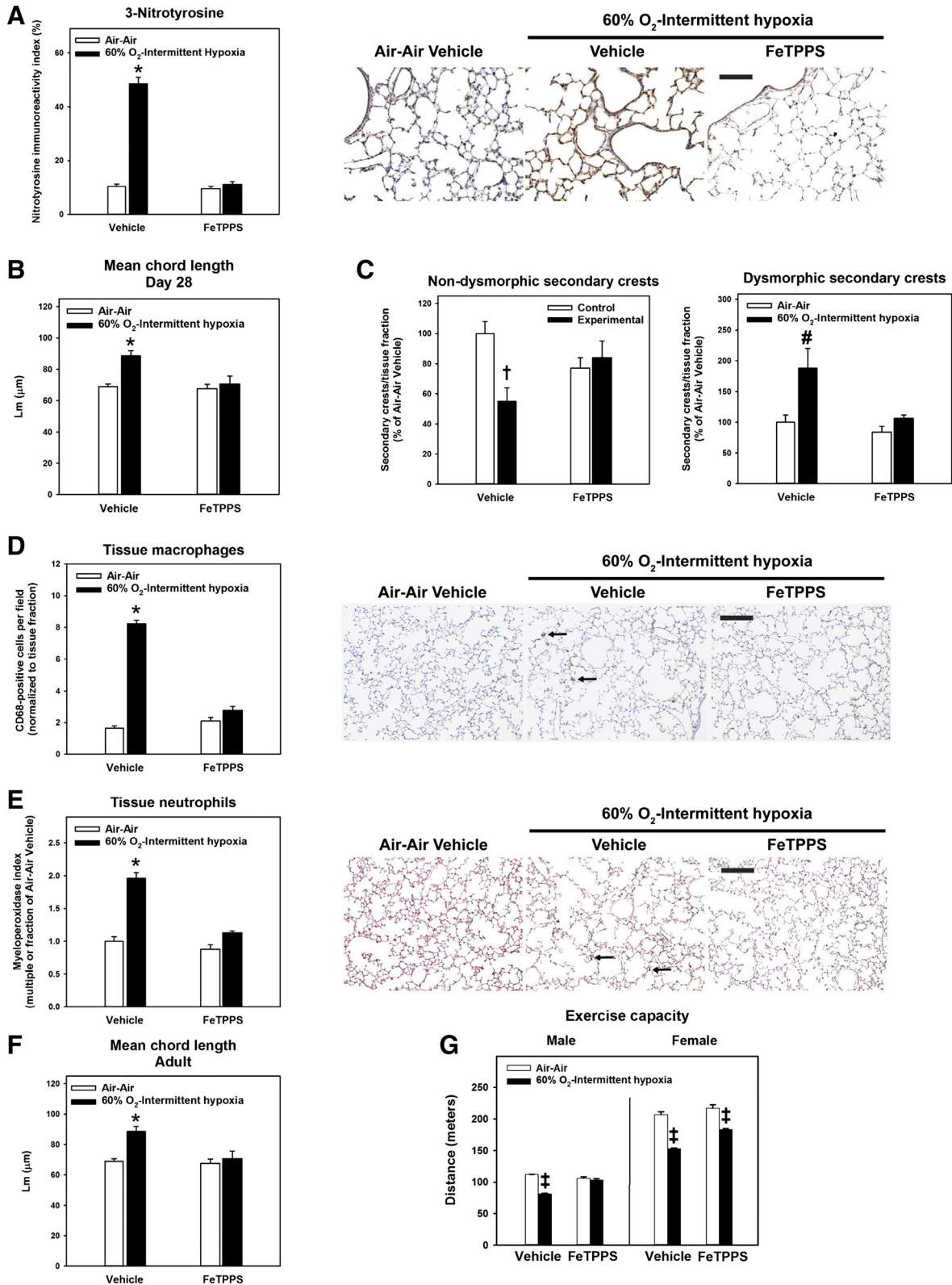


Fig. 4. Lung structure, pulmonary vascular reactivity, and exercise tolerance in early adulthood. Rat pups were exposed to normoxia (Air; open bars) or hyperoxia (60% O₂; closed bars) from *postnatal days 1 to 14* followed by recovery in normoxia (Air) or intermittent hypoxia (Intermittent hypoxia) until *postnatal day 28*. Thereafter, animals recovered in room air until early adulthood (12 wk). *A* and *B*: morphometric analyses of mean chord length (*A*) and peripheral artery counts (*B*). *C*: representative low-power photomicrographs of elastin-stained sections (bar length = 250 μm). *D*: pulmonary vascular resistance index following acute exposure to 10% O₂. *E*: exercise capacity. Bars represent means \pm SE for $n = 4-6$ animals/group. * $P < 0.001$, by ANOVA, compared with all other groups. # $P < 0.05$, by ANOVA, compared with Air-Air group. † $P < 0.05$, by ANOVA, compared with Air-Air and 60% O₂-Air groups. ‡ $P < 0.05$, by ANOVA, compared with Air-Air and 60% O₂-Air groups for the same sex. ¶ $P < 0.001$, by ANOVA, compared with all other groups for the same sex.

decreased in both male and female young adult animals exposed to 60% O₂-IH (Fig. 4E). Body weight has been shown in rats to greatly influence endurance, independent of sex (12). Therefore, a likely contributing factor to the sex difference in exercise capacity was the greater body weight of males

(358 ± 5 vs. 233 ± 5 g for females; *P* < 0.001 by *t*-test). In accord, distance run was no longer significantly different between sexes when indexed to body weight (data not shown). There were no differences in body weight within either sex between exposure groups (*P* > 0.05; data not shown).



Treatment with the peroxynitrite decomposition catalyst FeTPPS prevents lung structural changes, lung inflammation, and impaired exercise tolerance secondary to IH. Clinical and experimental evidence strongly implicates the reactive nitrogen species, peroxynitrite, as a critical mediator of chronic neonatal lung injury (6, 28). We treated a subset of animals with FeTPPS from PND 14 to 28 to determine the contribution of peroxynitrite to IH-mediated lung injury following exposure to 60% O₂. When compared with vehicle-treated animals at PND 28, treatment with FeTPPS reduced 3-nitrotyrosine immunoreactivity secondary to 60% O₂-IH (Fig. 5A), normalized L_m (Figs. 5B), and increased the proportion of nondysmorphic secondary crests (Fig. 5C). These effects were associated with attenuation of lung inflammation, with fewer tissue macrophages (Fig. 5D) and neutrophils (Fig. 5E). Preventive effects of FeTPPS extended into young adulthood, preserving L_m (Fig. 5F) and increasing exercise capacity (Fig. 5G).

DISCUSSION

Much of our understanding of the pathogenesis of BPD comes from animal models (19, 39). The usefulness of such models is in large part determined by the extent to which they replicate the pathophysiology in human infants (1). Unlike the original pathological description, so-called “new BPD” lacks the florid airway damage and fibrosis, characterized instead by arrested alveolar development. Term rodents are highly suitable as models for neonatal lung injury, since alveolar development is a postnatal event, as it is in prematurely born humans (35). Rats are the preferred rodent species for modeling chronic PHT associated with BPD, since vascular remodeling develops more readily than in mice (41). In addition, mice lack respiratory bronchioles, leading to a simplified acinar structure with fewer airway generations than in humans and rats (4). It is now recognized that inhibition of alveolar development in human neonates with BPD may be permanent and potentially progressive, thereby acting as an important antecedent for adult lung diseases such as COPD (33). Therefore, it is critical for animal models to replicate permanence of lung injury and for preclinical studies to incorporate examination of the long-term impact of interventions.

The major novel findings of this study were that arrest of alveologenesis secondary to 60% O₂ spontaneously resolves, which was prevented by a consecutive “second hit” with IH. Intermittent hypoxemic episodes are frequently observed in ex-premature infants with established or evolving BPD (17, 40). Changes lasting into young adulthood secondary to IH included persistent emphysematous lung structure, reduced vascularity, and decreased exercise capacity. Such changes are consistent with a permanent reduction of “lung units,” com-

prising alveoli and accompanying distal vessels, thus limiting respiratory capacity and reserve (5). In addition, while changes of chronic PHT improved over time, as reported in most children with BPD-associated PHT (10), we observed hyper-reactivity of the pulmonary vasculature to acute hypoxia, which has been described in young adult survivors of PPHN (37) and may also be present in childhood survivors of BPD (22). There were no apparent sex differences in the immediate or long-term effects of 60% O₂-IH on the above parameters (data not shown); however, we did not power the present study for the purpose of stratifying data by sex.

Mechanisms known to contribute to 60% O₂-induced lung injury include oxidative and nitrate stress, downstream of inflammatory cells and inflammatory mediators, including interleukin-1 and cyclooxygenase-2 (21, 28–31). In human infants with BPD, 3-nitrotyrosine levels (a stable marker of reactive nitrogen species, such as peroxynitrite) from circulating and lung-derived proteins are a direct marker of disease severity (6, 38). Our current findings employing FeTPPS indicate that peroxynitrite also plays a critical role in persistent lung inflammation and abnormal structure mediated by IH. Possible downstream effects of peroxynitrite-induced inhibition of alveologenesis, not yet explored, include nitration-mediated changes in expression and function of growth factors (7, 28) and mediators of angiogenesis (14, 28). Pulmonary vascular hyperreactivity has also been described in piglets exposed to brief postnatal hyperoxia, secondary to changes in thromboxane receptor function (20) and to increased oxidative stress (15).

In conclusion, exposure of juvenile rats to IH during recovery from hyperoxia-induced chronic neonatal lung injury caused abnormalities in lung structure and function to persist into young adulthood, thus more closely mimicking contemporary BPD. We propose that this model could be useful in deriving new insights into the pathogenesis of clinically relevant injuries and for preclinical studies incorporating examination of longevity of effects on lung structure and function.

GRANTS

This work was supported by operating funding from the Canadian Institutes of Health Research (MOP-84290 to R. P. Jankov and MOP-15276 to A. K. Tanswell) and by infrastructure funding from the Canada Foundation for Innovation (to R. P. Jankov). A. Mankouski was supported by a T32 award from the National Institute of Child Health and Human Development (4T32-HD-043029-14) and by grants from the Jean and George Brumley, Jr., Neonatal-Perinatal Research Institute and the Derfner-Children’s Miracle Network. A. Jain was supported by a Clinician-Scientist Training Program Award from the Hospital for Sick Children Research Training Centre and by a Queen Elizabeth II/Heart and Stroke Foundation of Ontario Graduate Scholarship in Science and Technology. M. J. Wong was supported by a Graduate Scholarship from the Department of Physiology, University of Toronto, and by a

Fig. 5. Effects of treatment with 5,10,15,20-tetrakis(4-sulfonatophenyl)-21H,23H-porphyrin iron (III) chloride (FeTPPS). Rat pups were exposed to normoxia from *postnatal days 1 to 28* (Control; open bars) or 60% O₂ from *postnatal days 1 to 14* followed by intermittent hypoxia from *postnatal days 14 to 28* (Experimental; closed bars). From *postnatal days 14 to 28*, pups received daily injections of vehicle or 30 mg·kg⁻¹·day⁻¹ FeTPPS. A: 3-nitrotyrosine immunostaining index and representative photomicrographs of 3-nitrotyrosine immunohistochemistry (immunoreactive 3-nitrotyrosine shown as brown stain; bar length = 100 μm). B–E: mean chord length (B) and counts of normal/dysmorphic secondary crests (C), tissue macrophages (D), and tissue neutrophils (E) at *day 28*. Representative photomicrographs of CD68- or myeloperoxidase-stained sections are shown below each graph [arrows pointing to macrophages (brown) or groups of neutrophils (black); bar lengths = 100 μm]. F and G: mean chord length (F) and exercise capacity (G) in young adult animals following recovery in room air until 12 wk of life. Bars represent means ± SE for *n* = 5–8 animals/group. **P* < 0.01, by ANOVA, compared with all other groups. #*P* < 0.05, by ANOVA, compared with all other groups. †*P* < 0.05, by ANOVA, compared with Air-Air-exposed, vehicle-treated group. ‡*P* < 0.05, by ANOVA, compared with all other groups for the same sex.

Lorne Phenix Graduate award from the Cardiovascular Sciences Collaborative Program, Faculty of Medicine, University of Toronto.

DISCLOSURES

No conflicts of interest, financial or otherwise, are declared by the authors.

AUTHOR CONTRIBUTIONS

A.M., C.K., M.J.W., J.I., A.J., E.J.B., and S.N.M. performed experiments; A.M., C.K., and R.P.J. analyzed data; A.M., R.L.A., and R.P.J. interpreted results of experiments; A.M. and R.P.J. prepared figures; A.M., R.L.A., and R.P.J. drafted manuscript; A.M., C.K., M.J.W., J.I., A.J., E.J.B., S.N.M., A.K.T., R.L.A., and R.P.J. edited and revised manuscript; A.M., C.K., M.J.W., J.I., A.J., E.J.B., S.N.M., A.K.T., R.L.A., and R.P.J. approved final version of manuscript.

REFERENCES

- Ambalavanan N, Morty RE. Searching for better animal models of BPD: a perspective. *Am J Physiol Lung Cell Mol Physiol* 311: L924–L927, 2016. doi:10.1152/ajplung.00355.2016.
- An HS, Bae EJ, Kim GB, Kwon BS, Beak JS, Kim EK, Kim HS, Choi JH, Noh CI, Yun YS. Pulmonary hypertension in preterm infants with bronchopulmonary dysplasia. *Korean Circ J* 40: 131–136, 2010. doi:10.4070/kcj.2010.40.3.131.
- Anderson PJ, Doyle LW. Neurodevelopmental outcome of bronchopulmonary dysplasia. *Semin Perinatol* 30: 227–232, 2006. doi:10.1053/j.sempri.2006.05.010.
- Bal HS, Ghoshal NG. Morphology of the terminal bronchiolar region of common laboratory mammals. *Lab Anim* 22: 76–82, 1988. doi:10.1258/002367788780746539.
- Balinotti JE, Tiller CJ, Llapur CJ, Jones MH, Kimmel RN, Coates CE, Katz BP, Nguyen JT, Tepper RS. Growth of the lung parenchyma early in life. *Am J Respir Crit Care Med* 179: 134–137, 2009. doi:10.1164/rccm.200808-1224OC.
- Banks BA, Ischiropoulos H, McClelland M, Ballard PL, Ballard RA. Plasma 3-nitrotyrosine is elevated in premature infants who develop bronchopulmonary dysplasia. *Pediatrics* 101: 870–874, 1998. doi:10.1542/peds.101.5.870.
- Belcastro R, Lopez L, Li J, Masood A, Tanswell AK. Chronic lung injury in the neonatal rat: up-regulation of TGF β 1 and nitration of IGF-R1 by peroxynitrite as likely contributors to impaired alveologenesis. *Free Radic Biol Med* 80: 1–11, 2015. doi:10.1016/j.freeradbiomed.2014.12.011.
- Bhat R, Salas AA, Foster C, Carlo WA, Ambalavanan N. Prospective analysis of pulmonary hypertension in extremely low birth weight infants. *Pediatrics* 129: e682–e689, 2012. doi:10.1542/peds.2011-1827.
- Coalson JJ. Pathology of new bronchopulmonary dysplasia. *Semin Neonatol* 8: 73–81, 2003. doi:10.1016/S1084-2756(02)00193-8.
- del Cerro MJ, Sabaté Rotés A, Cartón A, Deiros L, Bret M, Cordeiro M, Verdú C, Barrios MI, Albajara L, Gutierrez-Larraya F. Pulmonary hypertension in bronchopulmonary dysplasia: clinical findings, cardiovascular anomalies and outcomes. *Pediatr Pulmonol* 49: 49–59, 2014. doi:10.1002/ppul.22797.
- Dunlop K, Gosal K, Kantores C, Ivanovska J, Dhaliwal R, Desjardins JF, Connelly KA, Jain A, McNamara PJ, Jankov RP. Therapeutic hypercapnia prevents inhaled nitric oxide-induced right-ventricular systolic dysfunction in juvenile rats. *Free Radic Biol Med* 69: 35–49, 2014. doi:10.1016/j.freeradbiomed.2014.01.008.
- Durkot MJ, Francesconi RP, Hubbard RW. Effect of age, weight, and metabolic rate on endurance, hyperthermia, and heatstroke mortality in a small animal model. *Aviat Space Environ Med* 57: 974–979, 1986.
- Ee MT, Kantores C, Ivanovska J, Wong MJ, Jain A, Jankov RP. Leukotriene B₄ mediates macrophage influx and pulmonary hypertension in bleomycin-induced chronic neonatal lung injury. *Am J Physiol Lung Cell Mol Physiol* 311: L292–L302, 2016. doi:10.1152/ajplung.00120.2016.
- Elberson VD, Nielsen LC, Wang H, Kumar HS. Effects of intermittent hypoxia and hyperoxia on angiogenesis and lung development in newborn mice. *J Neonatal Perinatal Med* 8: 313–322, 2015. doi:10.3233/NPM-15814134.
- Fike CD, Slaughter JC, Kaplowitz MR, Zhang Y, Aschner JL. Reactive oxygen species from NADPH oxidase contribute to altered pulmonary vascular responses in piglets with chronic hypoxia-induced pulmonary hypertension. *Am J Physiol Lung Cell Mol Physiol* 295: L881–L888, 2008. doi:10.1152/ajplung.00047.2008.
- Frank L, Groseclose E. Oxygen toxicity in newborn rats: the adverse effects of undernutrition. *J Appl Physiol Respir Environ Exerc Physiol* 53: 1248–1255, 1982.
- Garg M, Kurzner SI, Bautista DB, Keens TG. Clinically unsuspected hypoxia during sleep and feeding in infants with bronchopulmonary dysplasia. *Pediatrics* 81: 635–642, 1988.
- Han RN, Buch S, Tseu I, Young J, Christie NA, Frndova H, Lye SJ, Post M, Tanswell AK. Changes in structure, mechanics, and insulin-like growth factor-related gene expression in the lungs of newborn rats exposed to air or 60% oxygen. *Pediatr Res* 39: 921–929, 1996. doi:10.1203/00006450-199606000-00001.
- Hilgendorff A, Reiss I, Ehrhardt H, Eickelberg O, Alvira CM. Chronic lung disease in the preterm infant. Lessons learned from animal models. *Am J Respir Cell Mol Biol* 50: 233–245, 2014. doi:10.1165/rcmb.2013-0014TR.
- Hinton M, Mellow L, Halayko AJ, Gutsol A, Dakshinamurti S. Hypoxia induces hypersensitivity and hyperreactivity to thromboxane receptor agonist in neonatal pulmonary arterial myocytes. *Am J Physiol Lung Cell Mol Physiol* 290: L375–L384, 2006. doi:10.1152/ajplung.00307.2005.
- Johnson BH, Yi M, Masood A, Belcastro R, Li J, Shek S, Kantores C, Jankov RP, Tanswell AK. A critical role for the IL-1 receptor in lung injury induced in neonatal rats by 60% O₂. *Pediatr Res* 66: 260–265, 2009. doi:10.1203/PDR.0b013e3181b1bcd2.
- Joshi S, Wilson DG, Kotecha S, Pickerd N, Fraser AG, Kotecha S. Cardiovascular function in children who had chronic lung disease of prematurity. *Arch Dis Child Fetal Neonatal Ed* 99: F373–F379, 2014. doi:10.1136/archdischild-2013-305185.
- Kantores C, McNamara PJ, Teixeira L, Engelberts D, Murthy P, Kavanagh BP, Jankov RP. Therapeutic hypercapnia prevents chronic hypoxia-induced pulmonary hypertension in the newborn rat. *Am J Physiol Lung Cell Mol Physiol* 291: L912–L922, 2006. doi:10.1152/ajplung.00480.2005.
- Knudsen L, Weibel ER, Gundersen HJ, Weinstein FV, Ochs M. Assessment of air space size characteristics by intercept (chord) measurement: an accurate and efficient stereological approach. *J Appl Physiol* (1985) 108: 412–421, 2010. doi:10.1152/jappphysiol.01100.2009.
- Landry JS, Tremblay GM, Li PZ, Wong C, Benedetti A, Taivassalo T. Lung Function and Bronchial Hyperresponsiveness in Adults Born Prematurely. A Cohort Study. *Ann Am Thorac Soc* 13: 17–24, 2016. doi:10.1513/AnnalsATS.201508-553OC.
- Lee AH, Dhaliwal R, Kantores C, Ivanovska J, Gosal K, McNamara PJ, Letarte M, Jankov RP. Rho-kinase inhibitor prevents bleomycin-induced injury in neonatal rats independent of effects on lung inflammation. *Am J Respir Cell Mol Biol* 50: 61–73, 2014. doi:10.1165/rcmb.2013-0131OC.
- Martin RJ, Di Fiore JM, Walsh MC. Hypoxic Episodes in Bronchopulmonary Dysplasia. *Clin Perinatol* 42: 825–838, 2015. doi:10.1016/j.clp.2015.08.009.
- Masood A, Belcastro R, Li J, Kantores C, Jankov RP, Tanswell AK. A peroxynitrite decomposition catalyst prevents 60% O₂-mediated rat chronic neonatal lung injury. *Free Radic Biol Med* 49: 1182–1191, 2010. doi:10.1016/j.freeradbiomed.2010.07.001.
- Masood A, Yi M, Belcastro R, Li J, Lopez L, Kantores C, Jankov RP, Tanswell AK. Neutrophil elastase-induced elastin degradation mediates macrophage influx and lung injury in 60% O₂-exposed neonatal rats. *Am J Physiol Lung Cell Mol Physiol* 309: L53–L62, 2015. doi:10.1152/ajplung.00298.2014.
- Masood A, Yi M, Lau M, Belcastro R, Li J, Kantores C, Pace-Asciak CR, Jankov RP, Tanswell AK. Cyclooxygenase-2 inhibition partially protects against 60% O₂-mediated lung injury in neonatal rats. *Pediatr Pulmonol* 49: 991–1002, 2014. doi:10.1002/ppul.22921.
- Masood A, Yi M, Lau M, Belcastro R, Shek S, Pan J, Kantores C, McNamara PJ, Kavanagh BP, Belik J, Jankov RP, Tanswell AK. Therapeutic effects of hypercapnia on chronic lung injury and vascular remodeling in neonatal rats. *Am J Physiol Lung Cell Mol Physiol* 297: L920–L930, 2009. doi:10.1152/ajplung.00139.2009.
- McEvoy CT, Jain L, Schmidt B, Abman S, Bancalari E, Aschner JL. Bronchopulmonary dysplasia: NHLBI Workshop on the Primary Prevention of Chronic Lung Diseases. *Ann Am Thorac Soc* 11, Suppl 3: S146–S153, 2014. doi:10.1513/AnnalsATS.201312-424LD.

33. **Meiners S, Hilgendorff A.** Early injury of the neonatal lung contributes to premature lung aging: a hypothesis. *Mol Cell Pediatr* 3: 24, 2016. doi:10.1186/s40348-016-0052-8.
34. **Nakanishi H, Uchiyama A, Kusuda S.** Impact of pulmonary hypertension on neurodevelopmental outcome in preterm infants with bronchopulmonary dysplasia: a cohort study. *J Perinatol* 36: 890–896, 2016. doi:10.1038/jp.2016.108.
35. **O'Reilly M, Thébaud B.** Animal models of bronchopulmonary dysplasia. The term rat models. *Am J Physiol Lung Cell Mol Physiol* 307: L948–L958, 2014. doi:10.1152/ajplung.00160.2014.
36. **Padela S, Cabacungan J, Shek S, Belcastro R, Yi M, Jankov RP, Tanswell AK.** Hepatocyte growth factor is required for alveologenesis in the neonatal rat. *Am J Respir Crit Care Med* 172: 907–914, 2005. doi:10.1164/rccm.200504-567OC.
37. **Sartori C, Allemann Y, Trueb L, Delabays A, Nicod P, Scherrer U.** Augmented vasoreactivity in adult life associated with perinatal vascular insult. *Lancet* 353: 2205–2207, 1999. doi:10.1016/S0140-6736(98)08352-4.
38. **Sheffield M, Mabry S, Thibeault DW, Truog WE.** Pulmonary nitric oxide synthases and nitrotyrosine: findings during lung development and in chronic lung disease of prematurity. *Pediatrics* 118: 1056–1064, 2006. doi:10.1542/peds.2006-0195.
39. **Silva DM, Nardiello C, Pozarska A, Morty RE.** Recent advances in the mechanisms of lung alveolarization and the pathogenesis of bronchopulmonary dysplasia. *Am J Physiol Lung Cell Mol Physiol* 309: L1239–L1272, 2015. doi:10.1152/ajplung.00268.2015. PubMed
40. **Singer L, Martin RJ, Hawkins SW, Benson-Szekely LJ, Yamashita TS, Carlo WA.** Oxygen desaturation complicates feeding in infants with bronchopulmonary dysplasia after discharge. *Pediatrics* 90: 380–384, 1992.
41. **Stenmark KR, Meyrick B, Galie N, Mooi WJ, McMurtry IF.** Animal models of pulmonary arterial hypertension: the hope for etiological discovery and pharmacological cure. *Am J Physiol Lung Cell Mol Physiol* 297: L1013–L1032, 2009. doi:10.1152/ajplung.00217.2009.
42. **Thibeault DW, Truog WE, Ekekezie II.** Acinar arterial changes with chronic lung disease of prematurity in the surfactant era. *Pediatr Pulmonol* 36: 482–489, 2003. doi:10.1002/ppul.10349.
43. **Vollsæter M, Clemm HH, Satrell E, Eide GE, Røksund OD, Markestad T, Halvorsen T.** Adult respiratory outcomes of extreme preterm birth. A regional cohort study. *Ann Am Thorac Soc* 12: 313–322, 2015. doi:10.1513/AnnalsATS.201406-285OC.
44. **Wedgwood S, Warford C, Agvateesiri SC, Thai P, Berkelhamer SK, Perez M, Underwood MA, Steinhorn RH.** Postnatal growth restriction augments oxygen-induced pulmonary hypertension in a neonatal rat model of bronchopulmonary dysplasia. *Pediatr Res* 80: 894–902, 2016. doi:10.1038/pr.2016.164.
45. **Weibel ER.** *Morphometry of the human lung.* Berlin: Springer Verlag, 1963. doi:10.1007/978-3-642-87553-3.
46. **Wong MJ, Kantores C, Ivanovska J, Jain A, Jankov RP.** Simvastatin prevents and reverses chronic pulmonary hypertension in newborn rats via pleiotropic inhibition of RhoA signaling. *Am J Physiol Lung Cell Mol Physiol* 311: L985–L999, 2016. doi:10.1152/ajplung.00345.2016.
47. **Wong PM, Lees AN, Louw J, Lee FY, French N, Gain K, Murray CP, Wilson A, Chambers DC.** Emphysema in young adult survivors of moderate-to-severe bronchopulmonary dysplasia. *Eur Respir J* 32: 321–328, 2008. doi:10.1183/09031936.00127107.

